

QCD相变的戴森-施温格方程方法研究

高飞¹ 刘玉鑫²

1(北京理工大学 物理学院 北京 100081)

2(北京大学 物理学院 北京 100871)

摘要 量子色动力学(Quantum Chromodynamics, QCD)在有限温度有限密度平面内具有丰富的相结构, 关于相边界曲线、临界终点(Critical Endpoint, CEP)的位置以及各相的热力学性质、状态方程等的研究是目前理论和实验上的重点问题, 寻找QCD相变信号, 特别是确定CEP的位置, 成为了相对论性重离子对撞机当前和未来实验计划的主要目标。本文简要小结在QCD的戴森-施温格方程(Dyson-Schwinger equation, DSE)方法框架下, 关于手征对称性恢复相变和退禁闭相变研究的进展和主要结果, 着重介绍关于DSE的截断方案的探索和完善、QCD相变的手征磁化率判据和推广的施温格(Schwinger)函数判据、及由之确定的手征和禁闭两种相变的相图。DSE方法预言的手征相变的CEP位置大致位于(T, μ_B) (110, 600) MeV, 与泛函重整化群等方法预言的结果一致。这些结果对于重离子对撞实验搜寻CEP信号具有指导价值。

关键词 QCD相变, 手征对称性动力学破缺, 解禁闭, 戴森-施温格方程, 手征磁化率

中图分类号 TL99

DOI: 10.11889/j.0253-3219.2023.hjs.46.040015

QCD phase transitions using the QCD Dyson-Schwinger equation approach

GAO Fei¹ LIU Yuxin²

1(School of Physics, Beijing Institution of Technology, Beijing 100081, China)

2(School of Physics, Peking University, Beijing 100871, China)

Abstract The use of the relativistic heavy ion collision experiment has extended our insights into the diverse possibilities available to a truly strongly-interacting system. The main goal of this experiment is to describe the properties of the different phases of quantum chromodynamics (QCD) and to chart the QCD phase diagram on the T - μ plane. For the phase diagram, apart from the general phase boundary lines, some specific characteristics such as the possible critical endpoint (CEP), associated coexistence region, and strongly-coupling quark-gluon plasma (sQGP) have to be identified. Here, the CEP separates the first-order phase transition from the second-order transition (or crossover) when the case beyond the chiral limit is considered. However, convincing signals have not yet been obtained using the relativistic heavy ion collider (RHIC) experiment. Theoretically, strong interaction systems hold significant features: asymptotic freedom in the ultraviolet region, dynamical chiral symmetry breaking, and confinement in the infrared region. Such features can be uniformly displayed in the phase structure of the matter in the temperature T and chemical potential planes. Consequently, several investigations have been experimentally and theoretically performed. However, the strong coupling feature in the low-energy region prevents the use of perturbative calculation methods, which creates the need for the development of nonperturbative approaches. Additionally, lattice QCD simulations have been widely implemented; however, the "sign problem" delays the

国家自然科学基金(No.11175004, No.12175007)资助

第一作者: 高飞, 男, 1989年出生, 2015年于北京大学获博士学位, 研究领域为中高能核物理, E-mail: fei.gao@bit.edu.cn

收稿日期: 2023-04-04, 修回日期: 2023-04-08

Supported by National Natural Science Foundation of China (No.11175004, No.12175007)

First author: GAO Fei, male, born in 1989, graduated from Peking University with a doctoral degree in 2015, focusing on medium and high energy nuclear physics, E-mail: fei.gao@bit.edu.cn

Received date: 2023-04-04, revised date: 2023-04-08

progress in the large chemical potential region. Therefore, the Dyson-Schwinger equation (DSE) equation method and functional renormalization group approach, which inherently include both dynamical chiral symmetry breaking (DCSB) and confinement, play an important role. The QCD DSE approach is a method based on the continuum quantum field theory. The new criteria were proposed based on the DSE and studied using the deconfinement and Chiral symmetry restoration phase transition of QCD. Currently, functional methods can be used to provide a reliable estimation of the CEP location. First, reliability is achieved using a thorough investigation of the truncation of the DSE, state of the art truncation is then performed causing a converging result between the different methods, and the prediction of the lattice simulation at low chemical potential is confirmed. The results show a fast convergence of the truncation owing to the infrared fixed point of the QCD coupling, which allows the capturing of the QCD running behavior using a finite set of two- and three-point Green functions. The estimated location of the CEP based on the current computation is μ_B at 600~650 MeV and T at 100~110 MeV. The existing functional QCD methods are non-perturbative continuum methods that are capable of simultaneously describing both the DCSB and confinement. Although they are limited by the truncations, the use of functional QCD approaches has resulted in progress in the study of the QCD phase structure and thermal properties, where a complete phase diagram and related thermal properties have been obtained in a large chemical potential range, which can provide a reference for the exploration of the QCD features. Most of the theoretical studies using effective models or certain truncations have observed the existence of the CEP; however, the determination of its location is still a work in progress because it varies based on the computation. Moreover, searching for QCD phase transition signals, particularly the CEP, is the main goals of current and future experimental programs on the relativistic heavy ion collider.

Key words QCD phase transition, Dynamical chiral symmetry breaking, Deconfinement, Dyson-Schwinger equations, Chiral susceptibility

由物理学“见物讲理、依理造物”的学科性质和范畴知道,对我们所处宇宙中的可见物质及其质量的产生和演化的研究自然是物理学中最重要的课题。按照现在的认识,我们现在所处的宇宙起源于130多亿年之前的一次大爆炸,经过平稳演化阶段之后出现暴涨。相应于暴涨引起的温度降低和空间膨胀,不可分辨的夸克和电子等轻子出现;再经降温,夸克因获得不同的流质量而可以区分;再进一步降温,可见物质的主要组成成分——强子出现,相应的可见物质具有了质量。显然,可见物质的最底层的组分粒子是夸克和胶子,其产生与演化过程即夸克(胶子)物质的状态的演化过程。与统计物理学原理对应,这一过程即强相互作用物质(亦常简称核物质)的相变。由于表述强相互作用的基本规律的理论是量子色动力学(Quantum Chromodynamics, QCD),因此,该过程常被称为QCD相变。由目前认识的强子的线度和强子物理的基本原理知,发生QCD相变的能标在 10^2 MeV,也就是在QCD的典型的非微扰能区,因此,抽象来讲,早期宇宙强相互作用物质的演化乃强相互作用物质在能标跑动下展现出截然不同的自由度、涌现出丰富而复杂的现象的表现。较具体地,这一演化即强相互作用物质随着温度密度变化由不禁闭不可见的具有手征对称性的夸克胶子相到色禁闭的手征对称性力学破缺的可见的强子相的相变过程^[1-7]。由此可知,研究QCD

相变及有限温度密度下各相物质的状态和性质将深化我们关于强相互作用基本规律的认识,并揭示可见物质及其质量起源的奥秘^[8-12]。

由于QCD相变是发生在QCD的非微扰能区的夸克胶子物质的状态演化现象,因此,人们利用相对论性重离子对撞对之进行实验研究、利用非微扰QCD方法对之进行理论研究。目前,理论上发展起来的非微扰QCD方法有离散场论层次上的格点QCD模拟方法、连续场论层次上的戴森-施温格方程(Dyson-Schwinger Equation, DSE)方法和泛函重整化群(Functional Renormalization Group, fRG)方法及多种唯象模型方法。经过50年的努力,理论和实验对于有限温度密度的QCD相变和相图的研究都取得了很大的进展^[13-16]。一般而言,在温度密度平面上,QCD相变分为两种:手征对称性破缺与手征对称性恢复之间的相变(常简称为手征相变)、禁闭与退禁闭之间的相变(禁闭相变)。两种相变在不同的判据下表现并不相同。在零化学势下的格点QCD模拟计算^[17-18]中,使用Polyakov圈判据发现两种相变具有较好的一致性,而在DSE的计算却给出Polyakov圈在有限密度区域退禁闭相变较手征相变温度仍会有一定差别的结论^[19],退禁闭温度略高于手征相变温度,出现“quarkyonic”相,这与大 N_c 极限下的一般分析的结论一致^[20]。但是通过对夸克传播子谱函数正定性的分析则得到轻味系统的手征相变

与退禁闭相变一致的结论^[21-23],关于关联函数的计算和分析也说明退禁闭温度相变温度与手征相变温度相同与否依赖于系统的味道^[24]。

考虑到对手征相变的定义及性质的描述非常清晰并且是QCD相变的主要模式,因此人们对手征相变的相图已进行了大量的理论研究^[25-72]。在高温低化学势情况下,格点QCD模拟和DSE方法等的计算都表明以温度为主要因素驱动的QCD的手征相变为连续过渡^[73-81]。然而,由于符号问题,格点QCD很难探索大化学势的区域,因此关于大化学势情况下的临界终点(Critical Endpoint, CEP)和一阶相变区域的存在性的研究主要是通过连续场论层次上的DSEs^[82-85]和fRG^[86-87]的泛函QCD方法来实现。泛函QCD方法是不仅是能够同时描述手征对称性动力学破缺(Dynamical Chiral Symmetry Breaking, DCSB)和禁闭的非微扰连续方法,还可以覆盖大范围的化学势区域,因此在研究QCD相变研究方面已取得了丰硕的进展^[88-91]。结果表明:在较大化学势下,以化学势为主要因素驱动的相变是一级相变,在确定相边界平衡曲线同时,这些计算也确认了连续过渡与一级相变的分界状态,即CEP。本文对DSE方法下关于QCD相变研究的方案、核心技术与难点,以及取得进展等予以简要介绍。

1 Dyson-Schwinger(DS)方程方法在QCD相变中的应用

1.1 DS方程的一般形式

Dyson-Schwinger(DS)方程是场论中关于格林函数的运动方程,最早由Dyson和Schwinger建立。通过DS方程可以得到场的格林函数,进而得到所有的可观测量。QCD的DS方程既能体现QCD的手征对称性动力学破缺又能体现色禁闭,是一种具有很好的普适性和QCD基础的非微扰连续场论方法,在对强相互作用系统的研究中取得了许多有意义的结果。为了得到量子场的DS方程,首先需要给出场的生成泛函。引入鬼场后,QCD的Faddeev-Popov拉式量为:

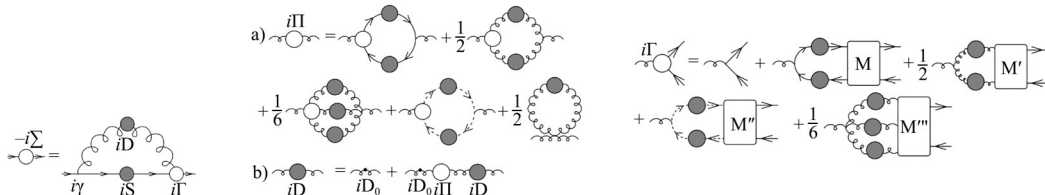


图1 夸克、胶子、夸克胶子顶点的DSE方程的费曼图表示

Fig.1 Feynman diagram for the DSE of the quark, gluon, and quark-gluon interaction vertex

$$\mathcal{L} = -\frac{1}{4}(F_{\mu\nu}^a)^2 - \frac{1}{2\xi}(\partial^\mu A_\mu^a)^2 + \bar{\psi}(i\dot{D} - m)\psi + \bar{c}^a(-\partial^\mu D_\mu^{ac})c^c \quad (1)$$

其中: $D_\mu = \partial_\mu - igA_\mu^at^a$, $D_\mu^{ac} = \partial_\mu\delta^{ac} - igA_\mu^bf^{bac}$, $F_{\mu\nu}^a = \partial_\mu A_\nu^a - \partial_\nu A_\mu^a + gf^{abc}A_\mu^bA_\nu^c$ 。

由此可以得到生成泛函为:

$$Z = \int d\mu e^{iS + i\int (\bar{\eta}\psi + \bar{\psi}\eta + J^a \cdot A^a + \bar{c}^a \bar{c}^a + \bar{\xi}^a c^a) d^4y} \quad (2)$$

$$d\mu = D\psi D\bar{\psi} DA_\mu^a Dc^b D\bar{c}^c$$

基于对生成泛函的泛函积分内对某场的变分为零,例如:

$$\int d\mu \frac{\delta}{\delta A_\mu} e^{iS + i\int (\bar{\eta}\psi + \bar{\psi}\eta + J \cdot A) d^4y} = 0 \quad (3)$$

即得相应场的DS方程。

DS方程是一组包含无穷多个积分方程的不封闭的方程组,它们由不同阶的格林函数耦合而成。在实际应用中,人们需要引入一定的截断方案才能对DS方程进行求解。原则上,所有的观测量均可从格林函数中提取出来,将QCD的作用量代入,并求解相应的DS方程即可得到QCD的所有物理性质。考虑到QCD作用量的具体形式, n 点的格林函数的DS方程会包含 $(n+1)$ 点和 $(n+2)$ 点的格林函数,而且越高阶的格林函数的DS方程形式越复杂。因此通常情况下,可以采取一些合理的截断方案,只求解最低阶格林函数的DS方程。为了得到关于手征对称性破缺以及禁闭的信息,通常用到的是最低阶的夸克胶子传播子和夸克胶子顶点的DS方程、相应的夸克和胶子以及顶点的费曼图如图1所示。

为了研究QCD物质在有限温度密度下的相图,还需要根据有限温度场论的原理引入温度和密度自由度。如果仅考虑平衡态的信息和平衡态相变,例如相图以及压强、能量密度、熵密度等热力学性质时,仅需要引入虚时温度场论,并以粒子的化学势表征相应粒子的密度。对于系统的演化信息以及输运性质等非平衡态的信息,则需要实时温度场论,即Schwinger-Keldysh形式。本文仅介绍关于QCD相图的研究,因此局限于虚时温度场论的内容。首先,考虑平衡体系的算符 \hat{A} 的平均值为:

$$\frac{1}{Z} \text{Tr} \left(e^{-\beta(\hat{H} - \mu \hat{N})} \hat{A} \right)$$

其中: $Z = \text{Tr} \left(e^{-\beta(\hat{H} - \mu \hat{N})} \right)$ 即系统的配分函数。可以看到, 配分函数的形式与路径积分非常相似:

$$\begin{aligned} \text{Tr} \left(e^{-\beta \hat{H}} \hat{A} \right) &= \int d\phi \left\langle \phi \left| e^{-\beta \hat{H}} (-i\beta) \hat{A} \right| \phi \right\rangle \\ &= \int D[\phi] e^{\int_0^\beta dt / d\bar{x} \mathcal{L}^{[\phi(t, \bar{x})]}} A[\phi] \\ &= \int D[\phi] e^{\int_0^\beta dt / d\bar{x} \mathcal{L}^{[\phi(t, \bar{x})]}} A[\phi] \end{aligned} \quad (4)$$

这表明, 配分函数相当于虚时空间的路径积分, 虚时 $\tau \in [0, \beta]$ 。配分函数中的求迹为场带来边界条件。对玻色子, 有格林函数:

$$\begin{aligned} G(\vec{x}, \vec{y}; t, 0) &= \frac{1}{T r e^{-\beta \hat{H}}} T r e^{-\beta \hat{H}} T \left[\hat{\phi}(\vec{x}, t) \hat{\phi}(\vec{y}, 0) \right] \\ &= \frac{1}{Z} T r \hat{\phi}(\vec{x}, t) e^{-\beta \hat{H}} e^{\beta \hat{H}} \hat{\phi}(\vec{y}, 0) e^{-\beta \hat{H}} \\ &= \frac{1}{Z} T r e^{-\beta \hat{H}} \hat{\phi}(\vec{y}, \beta) \hat{\phi}(\vec{x}, t) \\ &= \frac{1}{Z} T r e^{-\beta \hat{H}} T \left[\hat{\phi}(\vec{x}, t) \hat{\phi}(\vec{y}, \beta) \right] \end{aligned} \quad (5)$$

得到 $\hat{\phi}(\vec{y}, \beta) = \hat{\phi}(\vec{y}, 0)$, 对虚时的 $\phi(\vec{x}, \tau)$ 作傅里叶变换得到动量空间中的 $\tilde{\phi}(\vec{p}, \omega_n)$:

$$\phi(\vec{x}, \tau) = \frac{1}{\beta} \sum_n \int \frac{d\vec{p}}{(2\pi)^3} \tilde{\phi}(\vec{p}, \omega_n) e^{i(\vec{p} \cdot \vec{x} + \omega_n \tau)} \quad (6)$$

由周期边界条件得: $\omega_n = 2\pi n T$ 。

对于费米子, 最后一步交换 $\bar{\psi}(x)$ 与 $\psi(y)$ 会产生负号, 所以 $\psi(\vec{y}, \beta) = -\psi(\vec{y}, 0)$, 于是:

$$\begin{aligned} \psi(\vec{x}, \tau) &= \frac{1}{\beta} \sum_n \int \frac{d\vec{p}}{(2\pi)^3} \tilde{\psi}(\vec{p}, \omega_n) e^{i(\vec{p} \cdot \vec{x} + \omega_n \tau)} \\ \omega_n &= (2n + 1)\pi T \end{aligned} \quad (7)$$

由此, 前述零温零密的方法依旧适用于处于平衡态的有限温度有限密度体系, 仅 $O(4)$ 对称性退化成 $O(3)$ 对称性, 相应的传播子以及顶点的形式变为 $O(3)$ 的参数化形式。

1.2 夸克胶子传播子的 gap 方程及其解的一般性质与相变判据

为了得到 QCD 的相图, 我们需要对夸克胶子传播子以及夸克胶子顶点按照洛伦茨结构进行分解才能数值求解。其中, 夸克传播子可以写为:

$$\begin{aligned} S(\vec{p}, \tilde{\omega}_k) &= \\ &\left[i\gamma \cdot \vec{p} A(\vec{p}^2, \tilde{\omega}_k^2) + B(\vec{p}^2, \tilde{\omega}_k^2) + i\gamma_4 \tilde{\omega}_k C(\vec{p}^2, \tilde{\omega}_k^2) \right]^{-1} \end{aligned} \quad (8)$$

相应的胶子传播子为:

$$g^2 D_{\mu\nu}(p_{\Omega_k}) = P_{\mu\nu}^L(p_{\Omega_k}) \Delta_F(p_{\Omega_k}) + P_{\mu\nu}^T(p_{\Omega_k}) \Delta_G(p_{\Omega_k}) \quad (9)$$

其中: $p_{\Omega_k} = (\vec{p}, \Omega_k)$, $\Omega_k = 2k\pi T$, $P_{\mu\nu}^L$ 、 $P_{\mu\nu}^T$ 分别是 $\delta_{\mu\nu}$ - $\frac{p_\mu p_\nu}{p^2}$ 的三动量和能量分量:

$$\begin{aligned} P_{\mu\nu}^T(p_{\Omega_k}) &= \begin{cases} 0, & \mu, \nu = 4 \\ \delta_{ij} - \frac{p_i p_j}{p^2}, & \mu, \nu = i, j = 1, 2, 3 \end{cases} \\ P_{\mu\nu}^L(p_{\Omega_k}) &= \delta_{\mu\nu} - \frac{p_\mu p_\nu}{p^2} - P_{\mu\nu}^T(p_{\Omega_k}) \end{aligned} \quad (10)$$

为具体求解夸克传播子的 gap 方程, 我们需要对夸克胶子顶点进行一定的截断。关于夸克胶子顶点的截断方案决定了 DSE 方程方法的可靠性, 也是目前 DSE 方程方法研究最重要的部分。从洛伦兹结构来说, 顶点横向部分可以写为: $\Gamma_t^\mu = \tau_i(q^2, p^2, k^2) T_i^\mu$, 其中 T_i^μ 是一组完备基^[92-95], 顶点纵向部分有 4 项, 可由瓦得-高桥恒等式 (Ward-Takahashi Identity, WTI) 完全约束为 Ball-Chiu 顶点, 一般表示为:

$$\begin{aligned} \Gamma_\mu^{\text{BC}}(\vec{q}, \omega_l, \vec{p}, \omega_n) &= \gamma_\mu^T \sum_A + \gamma_\mu^L \sum_C + \\ (p_n + q_l)_\mu \left[\frac{1}{2} \gamma_a^T (p_n + q_l)_a \Delta_A + \frac{1}{2} \gamma_a^L (p_n + q_l)_a \Delta_C - i \Delta_B \right] \end{aligned}$$

其中:

$$\begin{aligned} \sum_F(\vec{q}^2, \omega_l^2, \vec{p}^2, \omega_n^2) &= \frac{1}{2} [F(\vec{q}^2, \omega_l^2) + F(\vec{p}^2, \omega_n^2)] \\ \Delta_F(\vec{q}^2, \omega_l^2, \vec{p}^2, \omega_n^2) &= \frac{F(\vec{q}^2, \omega_l^2) - F(\vec{p}^2, \omega_n^2)}{q_l^2 - p_n^2} \end{aligned}$$

其中: $F=A, B, C$, $\gamma_\mu^T = \gamma_\mu - \gamma_\mu^L$, $\gamma_\mu^L = u_\mu \gamma_a u_a$, $u=(0, 0, 0, 1)$ 。

$$\begin{aligned} T_\mu^1(t, k) &= \frac{i}{2} (k^2 t_\mu - t \cdot k k_\mu) \\ T_\mu^2(t, k) &= \frac{i}{2} (k^2 t_\mu - t \cdot k k_\mu) \\ T_\mu^3(t, k) &= k^2 \gamma_\mu - k_\mu \dot{k} \\ T_\mu^4(t, k) &= \frac{i}{8} (k^2 t_\mu - t \cdot k k_\mu) (\dot{k}t - \dot{k}t) \\ T_\mu^5 &= \frac{i}{2} (\dot{k} \gamma_\mu - \gamma_\mu \dot{k}) = k_\nu \sigma_{\nu\mu} \\ T_\mu^6(t, k) &= t \cdot k \gamma_\mu - \dot{k} t_\mu \\ T_\mu^7(t, k) &= \frac{i}{2} t \cdot k (t_\mu - \gamma_\mu \dot{k}) + \frac{i}{4} t_\mu (\dot{k}t - \dot{k}t) \\ T_\mu^8(t, k) &= \frac{1}{2} (\dot{k} t_\mu - \dot{k} t_\mu) + \frac{\gamma_\mu}{4} (\dot{k}t - \dot{k}t) \\ k_\mu &= q_\mu - p_\mu, t_\mu = q_\mu + p_\mu \end{aligned} \quad (11)$$

目前的研究表明, 其中对 gap 方程贡献最重要的是 $T_\mu^3(t, k)$ 、 $T_\mu^5(t, k)$ 以及 $T_\mu^8(t, k)$ 三个结构, 其中 $T_\mu^3(t, k)$ 是顶点的领头阶结构, $T_\mu^5(t, k)$ 的结构来自于动力学质量的反常磁矩效应^[42], 同时也被横向 WTI

的研究进一步确认^[43],对于gap方程的贡献也尤其重要。目前来讲,大量研究基于裸顶点的截断方案,也就是彩虹-梯子近似方案,该方案可以保证基本的对称性,同时便于求解。然而,由于缺乏重要的 $T_\mu^5(t, k)$ 项,因此简单使用裸顶点不能自然地得到手征对称性动力学破缺。需要引入相互作用模型并采用较大的耦合常数才能在真空正确的层次上描述赝标和矢量介子等受对称性保护的强子的行为。而由于其并不能很好地描述相应的夸克胶子场的跑动行为,因此仅能定性地描述QCD相图。目前基于裸顶点的相互作用模型多采用Qin-Chang模型:

$$\mathcal{G}_{IR}(k^2) = \frac{8\pi^2}{\omega^4} D e^{-k^2/\omega^2} + \frac{8\pi^2 \gamma_m}{\ln \left[\tau + \left(1 + \frac{k^2}{\Lambda_{QCD}^2} \right)^2 \right]} (1 - e^{-k^2/4m_i^2})/k^2 \quad (12)$$

其中:第一项主要表征红外相互作用,耦合强度一般取为 $(D\omega)^{\frac{1}{3}} = 0.52$ GeV, $\omega=0.5$ GeV。第二项为紫外微扰项,其中 $\tau = e^2 - 1$, $m_i=0.5$ GeV, $\gamma_m = 12/25$, $\Lambda_{QCD}^2 = 0.234$ GeV。耦合强度的选取由真空下求解 π 和 ρ 介子质量以及衰变常数后与实验值对比来决定。

最新的研究表明^[38,41],如果同时考虑 $T_\mu^3(t, k)$ 、 $T_\mu^5(t, k)$ 以及 $T_\mu^8(t, k)$ 三个结构并封闭求解夸克胶子和夸克胶子顶点DSE时,QCD的跑动行为已经可以被很好地描述。因此,目前DSE方程关于QCD相图的研究已经可以定量地给出相变曲线以及CEP大概位置。这背后的深层原因是QCD耦合常数的红外固定点使得相互作用顶点处于近共形极限,这使得泛函QCD方法的截断方案趋于稳定,保证其在极大范围能标下均可以准确给出QCD基本场的跑动行为,从而统一自洽地描述强相互作用物质^[96]。这一现象可以从QCD的有效荷的计算中得到印证^[97]。图2给出了关于QCD有效荷的计算,其中实线和折线为DSE计算^[96],点线为全息QCD计算的结果^[97]。从图2可以看到,包含两点和三点格林函数跑动行为的DSE方程的解与实验观测的有效荷非常接近,因此,尽管DSE方程是一个无穷耦合的方程组,但是固定点的标度现象以及因此带来的在固定点附近可以微扰展开的事实使得高阶的格林函数对最终结果影响很小,因此,DSE方法的截断趋于封闭。

在截断方案确定之后DSE方程即可直接数值求解,进而给出手征对称性动力学破缺以及色禁闭

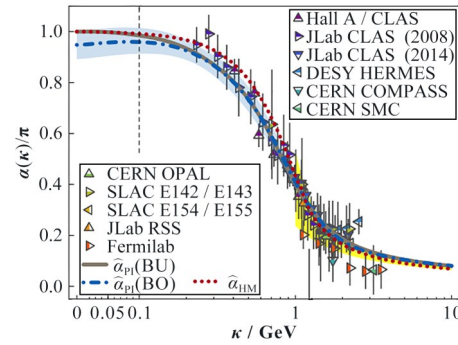


图2 过程不依赖的QCD有效荷^[97]
Fig.2 Process-independent effective charge^[97]

的性质。手征对称性动力学破缺与夸克传播子直接相关,在手征极限下,当夸克传播子的标量部分,也就是质量项不为零时为手征对称性破缺的Nambu相,质量项为零时为手征对称的Wigner相。因此,可以直接地定义零动量的质量函数 $B(p^2 = 0)$ 为手征极限下的序参量。更完整的序参量定义则是通过传播子求迹来定义手征凝聚:

$$\begin{aligned} -\langle \bar{q}q \rangle &= \int \text{tr}S(q) = \text{tr}_D \int \frac{d^4 p}{(2\pi)^4} S(p) \\ &= \int \frac{d^4 p}{(2\pi)^4} \frac{B(p^2)}{p^2 A^2(p^2) + B^2(p^2)} \end{aligned} \quad (13)$$

在手征极限下,手征凝聚是良好定义的。然而,在超越手征极限时,式中的积分发散,因此需要一定的减除方案。首先,利用求和规则可以给出质量函数在紫外的发散行为^[99-100]:

$$M(-Q^2) = \frac{B(-Q^2)}{A(-Q^2)} \xrightarrow{Q^2 \rightarrow \infty} \frac{c}{Q^2} [\ln(\frac{Q^2}{\Lambda_{QCD}^2})]^{m_0 - 1} + m_0 [\frac{\ln(\mu^2/\Lambda_{QCD}^2)}{\ln(Q^2/\Lambda_{QCD}^2)}]^{m_0} \quad (14)$$

因此,我们可以定义超越手征极限的序参量为:

$$\langle \bar{q}q \rangle = \langle \bar{q}q \rangle_{m_0} - m_0 \frac{\partial \langle \bar{q}q \rangle}{\partial m_0}_{m_0} \quad (15)$$

序参量可以通过磁化率结合热力学势给出相变的位置和相变级次。首先,热力学势可以展开为:

$$\Gamma(\langle \bar{q}q \rangle, \zeta) = \Gamma_0(\zeta) + \frac{1}{2} \alpha \langle \bar{q}q \rangle^2 + \frac{1}{4} \beta \langle \bar{q}q \rangle^4 + \frac{1}{6} \gamma \langle \bar{q}q \rangle^6 \quad (16)$$

定义磁化率为:

$$\chi = (\frac{\partial \langle \bar{q}q \rangle}{\partial \zeta})_{\zeta=\zeta_c} \quad (17)$$

则可以直接推导得到:

$$\begin{aligned}\chi &= \frac{-\langle \bar{q}q \rangle \left(\frac{\partial \alpha}{\partial \zeta} \right)_{\zeta=\zeta_c} - \langle \bar{q}q \rangle^3 \left(\frac{\partial \beta}{\partial \zeta} \right)_{\zeta=\zeta_c} - \langle \bar{q}q \rangle^5 \left(\frac{\partial \gamma}{\partial \zeta} \right)_{\zeta=\zeta_c}}{\alpha + 3\beta \langle \bar{q}q \rangle^2 + 5\gamma \langle \bar{q}q \rangle^4} \\ &= -\frac{\langle \bar{q}q \rangle \left(\frac{\partial \alpha}{\partial \zeta} \right)_{\zeta=\zeta_c} + \langle \bar{q}q \rangle^3 \left(\frac{\partial \beta}{\partial \zeta} \right)_{\zeta=\zeta_c} + \langle \bar{q}q \rangle^5 \left(\frac{\partial \gamma}{\partial \zeta} \right)_{\zeta=\zeta_c}}{\left(\frac{\partial^2 \Gamma}{\partial \langle \bar{q}q \rangle^2} \right)_{\frac{\partial \Gamma}{\partial \langle \bar{q}q \rangle}=0}}\end{aligned}\quad (18)$$

因此,当热力学势二阶导大于0,也就是系统相处于热力学势的极小值位置情况下,对于手征磁化率大于0的相为稳定相,对于磁化率小于0的相为不稳定相。两相共存时,磁化率较小的相认为是亚稳相。据此,利用磁化率判据,对完全非微扰因而无法确定系统热力学势的情况,我们也可以给出其手征相变的相边界曲线及CEP的状态。

关于禁闭,目前的判据主要在于胶子传播子以及相关的Polyakov势的结构,从夸克传播子判断禁闭的主要依据是夸克谱的正定性,首先夸克传播子可以表示为谱展开的形式即:

$$\begin{aligned}S(p) &= \int_0^\infty \frac{dM^2}{2\pi} \frac{\rho_s(M^2) - i\dot{p}\rho_v(M^2)}{p^2 + M^2} \\ \sigma(p^2) &= \int_0^\infty \frac{dM^2}{2\pi} \frac{\rho_s(M^2) - i\dot{p}\rho_v(M^2)}{p^2 + M^2} \\ &= \sigma_s(p^2) + \sigma_v(p^2)\end{aligned}\quad (19)$$

由于谱函数的信息需要实时温度场论,很难进行非微扰求解,因此,人们通常定义Schwinger函数来判断谱函数的正定性^[99]。在有限温度和密度下,可以通过传播子的谱表示定义如下的Schwinger函数:

$$d(P_N - P_W)/dT = \left(\partial P_N / \partial \mu - \partial P_W / \partial \mu \right) \partial \mu / \partial T + (\partial P_N / \partial T - \partial P_W / \partial T) = 0 \quad (22)$$

其中:压强对 μ 的导数即为粒子数密度 $\partial P_N / \partial \mu = n_N$,对 T 的导数为熵密度,即 $\partial P_N / \partial T = s_N$ 。一般来讲,手征对称性恢复的Wigner相的熵密度与粒子数密度均大于Nambu相的相应的值,由此我们得到相变曲线应满足如下关系:

$$\partial \mu / \partial T = -(s_N - s_W) / (n_N - n_W) < 0 \quad (23)$$

这表明随着化学势增大,相变温度会降低。同时,在小化学势区域可以对相变曲线按幂级数进行展开:

$$T_c(\mu_B) / T_c = 1 - \kappa(\mu_B / T_c)^2 + \lambda(\mu_B / T_c)^4 \quad (24)$$

通过上述分析可以看到, κ 应为正值。 κ 的具体数值决定相变曲线的主要行为,并且与QCD的跑动

$$\begin{aligned}\Delta(\tau, \vec{p} = 0) &= T \sum_n \int \frac{d^3 p}{(2\pi)^3} e^{-i(\tau \omega_n)} \sigma(p^2) \\ &= \frac{1}{2\pi} \int_{-\infty}^{\infty} d\omega \rho(\omega) \frac{e^{-(\omega + \mu)\tau}}{1 + e^{-(\omega + \mu)/T}}\end{aligned}\quad (20)$$

Schwinger函数的正定性是谱函数正定性的充分条件:如果谱函数是正定的,则Schwinger函数 $\Delta(\tau, \vec{p} = 0) \geq 0$;如果出现禁闭,谱函数存在负值,则Schwinger函数的正定性会被破坏。这一判据可以进一步推广^[101],直接数值求导可以看到Schwinger函数的 $2n$ 阶导数的正定性与谱函数的正定性保持一致:

$$\Delta^{2n}(\tau, \vec{p} = 0) = \frac{1}{2\pi} \int_{-\infty}^{\infty} d\omega (\omega + \mu)^{2n} \rho(\omega) \frac{e^{-(\omega + \mu)\tau}}{1 + e^{-(\omega + \mu)/T}} \quad (21)$$

因此,我们可以通过这一系列导数的正定性来判断谱函数的正定性,从而得到夸克禁闭的信息。

2 DS方程方法下的关于手征相变和退禁闭相变的主要结果

2.1 手征相变相图

首先,相边界曲线可以从热力学的角度进行一般的判断,考虑相变发生的位置位于两相压强相同的状态,即有 $P_N = P_W$,则有:

行为密切相关。目前格点QCD模拟给出对于2+1味的QCD系统, $\kappa \sim 0.015$,最新的DSE方法以及泛函重整化群方法也给出了一致的结果,表1给出目前不同QCD方法给出的最新结果的比较。

表1 相变曲线曲率 κ
Table 1 Curvature coefficients κ

计算方案 Methods	曲率 Coefficients κ
DSE ^[88-89]	0.015 0
DSE ^[55-56]	0.023 8
fRG ^[87]	0.014 2(2)
Lattice QCD ^[76]	0.015 3(18)
Lattice QCD ^[74]	0.014 4(26)
Lattice QCD ^[75]	0.015(451)

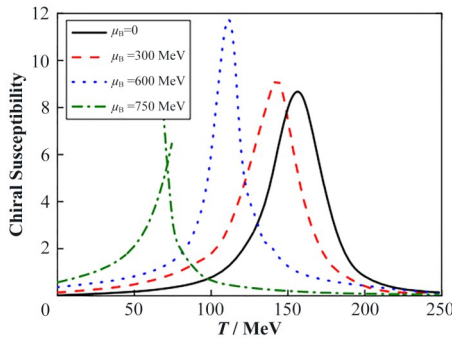


图3 一些不同化学势下,手征磁化率随温度变化的行为^[88]
Fig.3 T dependence of the chiral susceptibility at different chemical potentials^[88]

在整个温度化学势平面内数值求解夸克传播子的gap方程后可以直接带入手征磁化率的相变判据计算其随温度和化学势(密度)变化的行为。一些化学势下磁化率随温度变化的行为的结果如图3中展

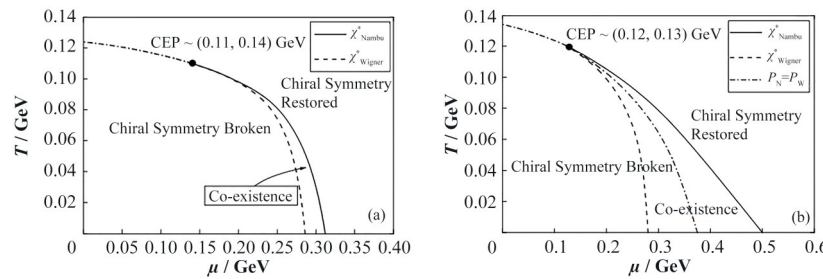


图4 QC胶子模型下,DS方程方法给出的QCD的手征相变的相图^[86]
Fig.4 QCD phase diagram under the QC interaction model using the QCD DS equation approach^[86]

目前,结合fRG方法的DS方程方法的最新计算给出了QCD的正确跑动行为。首先,在真空下夸克质量函数随动量的跑动行为与格点QCD模拟给出的结果一致;其次,在小化学势区域,相变温度与相变曲线的曲率也有格点QCD一致,相应的结果已列于表1中。因此,可以认为,目前的DS方程方法下的计算给出了关于QCD相变的可靠的结果。如图5所示,相关计算再次确认了CEP的存在,最新的计算给出CEP状态约位于 $(T, \mu_B) \sim (110, 600)$ MeV。

2.2 退禁闭相变相图

再者, DSE方程方法还给出了退禁闭相变相图的计算。在靠近相变温度时,Schwinger函数本身表现出正定性,但是Schwinger函数的高阶导数仍然出现了负值,最终如图6所示,Schwinger函数判据给出退禁闭相变与手征相变同时发生。另外,通过Polyakov圈对胶子传播子的计算也给出了相同的结论。尽管胶子部分在Polyakov圈中占据主要部分,但是相变的主要特征仍来源于夸克质量函数的

示。可以看到,在化学势较小的区域,手征磁化率是一个光滑函数,表明QCD相变实际是连续过渡,可以认为极大值的位置对应的温度即赝相变温度。随着化学势逐渐增大,磁化率趋于发散,发散的位置对应的状态即为CEP的状态。在更大的化学势处,磁化率断开,标志着系统进入一级相变区域。

首先,人们运用QC胶子模型对QCD的手征相变进行了大量的研究。由于截断方案的限制,相关的计算仅能定性确定QCD相变的行为。但是在不同的参数和方案下,相变曲线与CEP的位置均不尽相同,在一级相变区域,不同的方案给出的共存区大小也不尽一致。但是,这些计算仍然给出了一些确定的信息,首先,随着化学势增加,相变温度减小,这证实了前述的由热力学的一般讨论给出的结论;其次,所有的计算均一致地给出了CEP的存在,进一步给出了大化学势区域的共存区,相应地结果展示在图4中。

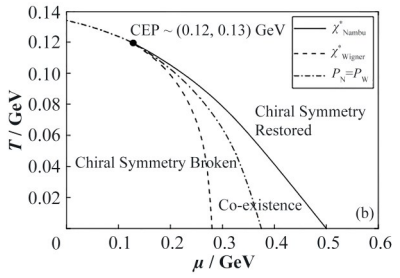


图5 QCD的DS方程方法最新给出的QCD的手征相变的相图^[89]
Fig.5 QCD phase diagram using the DS equation approach in the state of the art truncation scheme^[89]

变化。

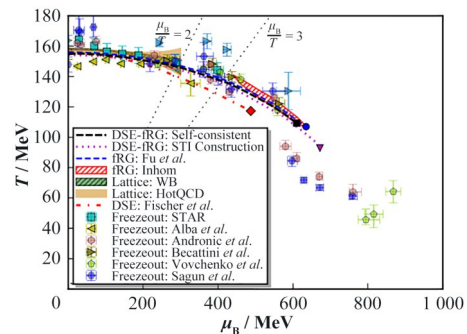
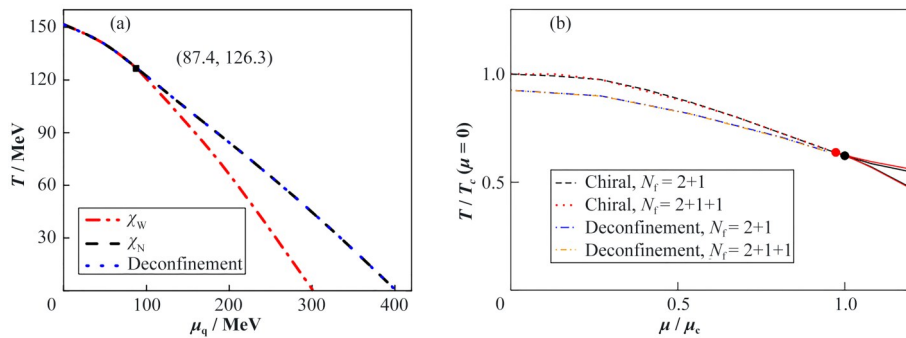


图5 QCD的DS方程方法最新给出的QCD的手征相变的相图^[89]
Fig.5 QCD phase diagram using the DS equation approach in the state of the art truncation scheme^[89]

3 QCD相变理论和实验现象研究的展望

我们知道,ALICE/CERN正在进行的实验计划和相对论重离子对撞器(Relativistic Heavy Ion Collider, RHIC)/布鲁克黑文国家实验室

图6 QCD退禁闭相变^[101] (a)Schwinger函数判据,(b)Polyakov势判据Fig.6 QCD deconfinement phase diagram under the criterion of Schwinger function (a) and Polyakov loop potential (b)^[101]

(Brookhaven National Laboratory, BNL)的能量扫描以及俄重离子同步加速器(Nuclotron-based Ion Collider facility, NICA)和HADES/CBM/FAIR及中国强流重离子加速器(High Intensity Heavy-ion Accelerator Facility, HIAF)的未来实验计划,都将搜寻QCD相变的CEP信号视为其主要任务。而如何从QCD的理论方法对QCD相图的结构和强相互作用物质的相关物理做出可靠的定性和定量预言是对目前理论研究的巨大挑战。其中,关于QCD的DS方程方法对QCD相结构的研究,已在本文中进行了回顾。原则上,DS方程方法对于QCD相变的研究可以实现两个本质上不同的目标:第一,它可以作为模型构建对QCD理论进行探索,对可能出现的QCD的新的物质状态和性质进行研究;第二,它可以通过完善截断方案来关注强相互作用的定量特征和现象学效应的探索。在本文中,我们给出了有限温度和化学势下DS方程方法的截断方案研究的进展以及相应的关于QCD相图的研究。目前的结果在零温以及低密区域已能给出与格点QCD模拟计算结果一致的结果,DS方程方法与泛函重整化群方法亦给出了一致的对CEP位置的预测。目前的研究表明,CEP的位置大致在温度局限在100~110 MeV内,化学势局限在600~650 MeV区间。需要指出的是,DS方程方法的截断方案在大化学势区域的可靠性仍需要进一步验证,特别是在顶点中强子和diquark道的贡献随着化学势增大不断增强,这也是下一步对截断方案进行改进的方向。对CEP位置的精确预言是未来一项重要且必要的工作。

关于QCD相变的理论研究和QCD的丰富的相结构的研究当然是今后研究的重点,例如手征相变与色禁闭相变的关系、由此可能产生的quarkyonic相的存在性以及产生机制的问题、强耦合夸克胶子等离子体相的激发模式、大化学势区域的色超导态、等。另外,加强理论探索与相对论性重离子碰撞实验物理的联系也是必须开展的工作。其中重要的接

口是重子数等守恒荷的涨落及其比率(已有初步结果^[102-103])、热力学量和输运系数,以及夸克、胶子和介子的谱函数的信息等。DSE方程方法在这方面已经迈出的有希望的一步,并将在未来发展扩大,对重离子碰撞的产物进行全方位的诠释。

致谢 感谢秦思学教授、付伟杰教授等的讨论和建议。

作者贡献说明 两位作者高飞、刘玉鑫共同负责编纂文章,整理文献等。

参考文献

- 1 Andronic A, Braun-Munzinger P, Redlich K, *et al.* Decoding the phase structure of QCD via particle production at high energy[J]. Nature, 2018, **561**(7723): 321 – 330. DOI: 10.1038/s41586-018-0491-6.
- 2 Edward S. Strongly coupled quark-gluon plasma in heavy ion collisions[J]. Reviews of Modern Physics, 2017, **89** (3): 035001.
- 3 Stephanov M A. Non-Gaussian fluctuations near the QCD critical point[J]. Physical Review Letters, 2009, **102**(3): 032301. DOI: 10.1103/PhysRevLett.102.032301.
- 4 Roberts C D, Schmidt S M. Dyson-Schwinger equations: density, temperature and continuum strong QCD[J]. Progress in Particle and Nuclear Physics, 2000, **45**: S1 – S103. DOI: 10.1016/S0146-6410(00)90011-5.
- 5 Fukushima K, Sasaki C. The phase diagram of nuclear and quark matter at high baryon density[J]. Progress in Particle and Nuclear Physics, 2013, **72**: 99 – 154. DOI: 10.1016/j.ppnp.2013.05.003.
- 6 Fischer C S. QCD at finite temperature and chemical potential from Dyson-Schwinger equations[J]. Progress in Particle and Nuclear Physics, 2019, **105**: 1 – 60. DOI: 10.1016/j.ppnp.2019.01.002.
- 7 Dupuis N, Canet L, Eichhorn A, *et al.* The

- nonperturbative functional renormalization group and its applications[J]. Physics Reports, 2021, **910**: 1 – 114. DOI: 10.1016/j.physrep.2021.01.001.
- 8 Adcox K, Adler S S, Afanasiev S, et al. Formation of dense partonic matter in relativistic nucleus-nucleus collisions at RHIC: experimental evaluation by the PHENIX Collaboration[J]. Nuclear Physics A, 2005, **757**(1 – 2): 184 – 283. DOI: 10.1016/j.nuclphysa.2005.03.086.
- 9 Arsene I, Bearden I G, Beavis D, et al. Quark-gluon plasma and color glass condensate at RHIC? The perspective from the BRAHMS experiment[J]. Nuclear Physics A, 2005, **757**(1 – 2): 1 – 27. DOI: 10.1016/j.nuclphysa.2005.02.130.
- 10 Adams J, Aggarwal M M, Ahammed Z, et al. Experimental and theoretical challenges in the search for the quark-gluon plasma: the STAR Collaboration's critical assessment of the evidence from RHIC collisions[J]. Nuclear Physics A, 2005, **757**(1 – 2): 102 – 183. DOI: 10.1016/j.nuclphysa.2005.03.085.
- 11 Boyanovsky D, De Vega H J, Schwarz D J. Phase transitions in the early and present universe[J]. Annual Review of Nuclear and Particle Science, 2006, **56**: 441 – 500.
- 12 Gao F, Oldengott I M. Cosmology meets functional QCD: first-order cosmic QCD transition induced by large lepton asymmetries[J]. Physical Review Letters, 2022, **128**(13): 131301.
- 13 DOE/NSF Nuclear Science Advisory Committee. The frontiers of nuclear science, a long range plan[EB/OL]. 2008: arXiv: 0809.3137. <https://arxiv.org/abs/0809.3137>.
- 14 Rajagopal K. Mapping the QCD phase diagram[J]. Nuclear Physics A, 1999, **661**(1 – 4): 150 – 161. DOI: 10.1016/S0375-9474(99)85017-9.
- 15 Braun-Munzinger P, Wambach J. Colloquium: Phase diagram of strongly interacting matter[J]. Reviews of Modern Physics, 2009, **81**(3): 1031 – 1050. DOI: 10.1103/RevModPhys.81.1031.
- 16 Fukushima K, Hatsuda T. The phase diagram of dense QCD[J]. Reports on Progress in Physics, 2011, **74**(1): 014001.
- 17 Cheng M, Christ N H, Datta S, et al. QCD equation of state with almost physical quark masses[J]. Physical Review D, 2008, **77**(1): 014511.
- 18 Bazavov A, Bhattacharya T, Cheng M, et al. Equation of state and QCD transition at finite temperature[J]. Physical Review D, 2009, **80**(1): 014504.
- 19 Fischer C S, Luecker J. Propagators and phase structure of $N_f=2$ and $N_f=2+1$ QCD[J]. Physics Letters B, 2013, **718**(3): 1036 – 1043.
- 20 McLerran L, Pisarski R D. Phases of dense quarks at large N_c [J]. Nuclear Physics A, 2007, **796**(1 – 4): 83 – 100.
- 21 Qin S, Rischke D H. Quark spectral function and deconfinement at nonzero temperature[J]. Physical Review D, 2013, **88**(5): 056007.
- 22 Karsch F, Kitazawa M. Quark propagator at finite temperature and finite momentum in quenched lattice QCD[J]. Physical Review D, 2009, **80**(5): 056001.
- 23 Mueller J A, Fischer C S, Nickel D. Quark spectral properties above T_c from Dyson-Schwinger equations[J]. The European Physical Journal C, 2010, **70**(4): 1037 – 1049. DOI: 10.1140/epjc/s10052-010-1499-8.
- 24 Chen L F, Qin S X, Liu Y X. Flavor dependence of the thermal dissociations of vector and axial-vector mesons [J]. Physical Review D, 2020, **102**(5): 054015.
- 25 Karsch F, Laermann E. Susceptibilities, the specific heat, and a cumulant in two-flavor QCD[J]. Physical Review D, Particles and Fields, 1994, **50**(11): 6954 – 6962. DOI: 10.1103/physrevd.50.6954.
- 26 Hatsuda T, Kunihiro T. QCD phenomenology based on a chiral effective Lagrangian[J]. Physics Reports, 1994, **247**(5 – 6): 221 – 367. DOI: 10.1016/0370-1573(94)90022-1.
- 27 Fodor Z, Katz S D. A new method to study lattice QCD at finite temperature and chemical potential[J]. Physics Letters B, 2002, **534**(1 – 4): 87 – 92. DOI: 10.1016/S0370-2693(02)01583-6.
- 28 de Forcrand P, Philipsen O. The QCD phase diagram for three degenerate flavors and small baryon density[J]. Nuclear Physics B, 2003, **673**(1 – 2): 170 – 186. DOI: 10.1016/j.nuclphysb.2003.09.005.
- 29 Fodor Z, Katz S D. Critical point of QCD at finite T and μ , lattice results for physical quark masses[J]. Journal of High Energy Physics, 2004, **2004**(04): 50.
- 30 D'Elia M, Lombardo M P. Finite density QCD via an imaginary chemical potential[J]. Physical Review D, 2003, **67**(1): 014505.
- 31 Bernard C, Burch T, DeTar C, et al. QCD thermodynamics with three flavors of improved staggered quarks[J]. Physical Review D, 2005, **71**(3): 034504.
- 32 Aoki Y, Endrődi G, Fodor Z, et al. The order of the quantum chromodynamics transition predicted by the standard model of particle physics[J]. Nature, 2006, **443**

- (7112): 675 – 678. DOI: 10.1038/nature05120.
- 33 Aoki Y, Fodor Z, Katz S D, *et al.* The QCD transition temperature: results with physical masses in the continuum limit[J]. Physics Letters B, 2006, **643**(1): 46 – 54. DOI: 10.1016/j.physletb.2006.10.021.
- 34 Gavai R V, Gupta S. On the critical end point of QCD[J]. Physical Review D, 2005, **71**(11): 114014
- 35 Gavai R V, Gupta S. QCD at finite chemical potential with six time slices[J]. Physical Review D, 2008, **78**(11): 114503.
- 36 Fodor Z, Katz S D. The phase diagram of quantum chromodynamics[EB/OL]. 2009: arXiv: 0908.3341. <https://arxiv.org/abs/0908.3341>.
- 37 de Forcrand P, Philipsen O. Constraining the QCD phase diagram by tricritical lines at imaginary chemical potential [J]. Physical Review Letters, 2010, **105**(15): 152001. DOI: 10.1103/PhysRevLett.105.152001.
- 38 Endrődi G, Fodor Z, Katz S D, *et al.* The QCD phase diagram at nonzero quark density[J]. Journal of High Energy Physics, 2011, **2011**(4): 1. DOI: 10.1007/JHEP04(2011)001.
- 39 Kaczmarek O, Karsch F, Laermann E, *et al.* Phase boundary for the chiral transition in (2+1)-flavor QCD at small values of the chemical potential[J]. Physical Review D - Particles, Fields, Gravitation and Cosmology, 2011, **83**(1): 014504.
- 40 Li A, Alexandru A, Liu K F. Critical point of $N_f = 3$ QCD from lattice simulations in the canonical ensemble[J]. Physical Review D, 2011, **84**(7): 071503.
- 41 Karsch F, Schaefer B J, Wagner M, *et al.* Towards finite density QCD with Taylor expansions[J]. Physics Letters B, 2011, **698**(3): 256 – 264.
- 42 Bhattacharya T, Buchoff M I, Christ N H, *et al.* QCD phase transition with chiral quarks and physical quark masses[J]. Physical Review Letters, 2014, **113**(8): 082001. DOI: 10.1103/PhysRevLett.113.082001.
- 43 Cea P, Cosmai L, Papa A. Critical line of 2+1 flavor QCD [J]. Physical Review D, 2014, **89**(7): 074512.
- 44 Gupta S, Karthik N, Majumdar P. On criticality and the equation of state of QCD at finite chemical potential[J]. Physical Review D, 2014, **90**(3): 034001.
- 45 Bhattacharya T, Buchoff M I, Christ N H, *et al.* QCD phase transition with chiral quarks and physical quark masses[J]. Physical Review Letters, 2014, **113**(8): 082001. DOI: 10.1103/PhysRevLett.113.082001.
- 46 Fischer C S, Mueller J A. Chiral and deconfinement transition from Dyson-Schwinger equations[J]. Physical Review D, 2009, **80**(7): 074029.
- 47 Isserstedt P, Buballa M, Fischer C S, *et al.* Baryon number fluctuations in the QCD phase diagram from Dyson-Schwinger equations[J]. Physical Review D, 2019, **100**(7): 074011.
- 48 Fu W, Luo X, Pawłowski J M, *et al.* Hyper-order baryon number fluctuations at finite temperature and density[J]. Physical Review D, 2021, **104**(9): 094047.
- 49 He M, Hu F, Sun W M, *et al.* Crossover from a continuum study of chiral susceptibility[J]. Physics Letters B, 2009, **675**(1): 32 – 37. DOI: 10.1016/j.physletb.2009.03.076.
- 50 Shi C, Wang Y L, Jiang Y, *et al.* Locate QCD critical end point in a continuum model study[J]. Journal of High Energy Physics, 2014, **2014**(7): 14. DOI: 10.1007/JHEP07(2014)014.
- 51 Xu S S, Cui Z F, Wang B, *et al.* Chiral phase transition with a chiral chemical potential in the framework of Dyson-Schwinger equations[J]. Physical Review D - Particles, Fields, Gravitation and Cosmology, 2015, **91**(5): 056003.
- 52 Lu Y, Cui Z F, Pan Z, *et al.* QCD phase diagram with a chiral chemical potential[J]. Physical Review D, 2016, **93**(7): 074037.
- 53 Gutiérrez E, Ahmad A, Ayala A, *et al.* The QCD phase diagram from Schwinger-Dyson equations[J]. Journal of Physics G: Nuclear and Particle Physics, 2014, **41**(7): 075002.
- 54 Fischer C S, Luecker J, Welzbacher C A. Phase structure of three and four flavor QCD[J]. Physical Review D, 2014, **90**(3): 034022.
- 55 Fischer C S, Luecker J, Welzbacher C A. Locating the critical end point of QCD[J]. Nuclear Physics A, 2014, **931**: 774 – 779.
- 56 Gao F, Chen J, Liu Y X, *et al.* Phase diagram and thermal properties of strong-interaction matter[J]. Physical Review D, 2016, **93**(9): 094019.
- 57 Hatta Y, Stephanov M A. Proton-number fluctuation as a signal of the QCD critical end point[J]. Physical Review Letters, 2003, **91**(10): 102003. DOI: 10.1103/PhysRevLett.91.102003.
- 58 Ghosh S K, Mukherjee T K, Mustafa M G, *et al.* Susceptibilities and speed of sound from the Polyakov-Nambu-Jona-Lasinio model[J]. Physical Review D, 2006, **73**(11): 114007.
- 59 Schaefer B J, Pawłowski J M, Wambach J. Phase

- structure of the Polyakov-quark-meson model[J]. Physical Review D, 2007, **76**(7): 074023.
- 60 Schaefer B J, Wagner M. Three-flavor chiral phase structure in hot and dense QCD matter[J]. Physical Review D, 2009, **79**(1): 014018.
- 61 Sasaki C, Friman B, Redlich K. Susceptibilities and the phase structure of a chiral model with Polyakov loops[J]. Physical Review D, 2007, **75**(7): 074013.
- 62 Fu W J, Zhang Z, Liu Y X. 2+1 Flavor Polyakov-Nambu-Jona-Lasinio model at finite temperature and nonzero chemical potential[J]. Physical Review D - Particles, Fields, Gravitation and Cosmology, 2008, **77**(1): 014006.
- 63 Ciminale M, Gatto R, Ippolito N D, et al. Three flavor Nambu-Jona-Lasinio model with Polyakov loop and competition with nuclear matter[J]. Physical Review D, 2008, **77**(5): 054023.
- 64 Sasaki C, Friman B, Redlich K. Chiral phase transition in the presence of spinodal decomposition[J]. Physical Review D, 2008, **77**(3): 034024. DOI: 10.1103/physrevd.77.034024.
- 65 Costa P, Ruivo M C, de Sousa C A. Thermodynamics and critical behavior in the Nambu-Jona-Lasinio model of QCD[J]. Physical Review D, 2008, **77**(9): 096001.
- 66 Fukushima K. Phase diagrams in the three-flavor Nambu-Jona-Lasinio model with the Polyakov loop[J]. Physical Review D, 2008, **77**(11): 114028.
- 67 Abuki H, Anglani R, Gatto R, et al. Chiral crossover, deconfinement, and quarkyonic matter within a Nambu-Jona-Lasinio model with the Polyakov loop[J]. Physical Review D, 2008, **78**(3): 034034.
- 68 Mao H, Jin J S, Huang M. Phase diagram and thermodynamics of the Polyakov linear sigma model with three quark flavors[J]. Journal of Physics G: Nuclear and Particle Physics, 2010, **37**(3): 035001.
- 69 Xin X Y, Qin S X, Liu Y X. Improvement on the Polyakov-Nambu-Jona-Lasinio model and the QCD phase transitions[J]. Physical Review D, 2014, **89**(9): 094012.
- 70 Chen X, Li D N, Huang M. Criticality of QCD in a holographic QCD model with critical end point[J]. Chinese Physics C, 2019, **43**(2): 023105.
- 71 Huang M. QCD phase diagram at high temperature and density[EB/OL]. 2010: arXiv: 1001.3216. <https://arxiv.org/abs/1001.3216>.
- 72 Zhao Y, Chang L, Yuan W, et al. Chiral susceptibility and chiral phase transition in Nambu-Jona-Lasinio model[J]. The European Physical Journal C, 2008, **56**(4): 483 - 492.
- DOI: 10.1140/epjc/s10052-008-0673-8.
- 73 Jiang L, Xin X, Wang K, et al. Revisiting the phase diagram of the three-flavor quark system in the Nambu-Jona-Lasinio model[J]. Physical Review D, 2013, **88**(1): 016008.
- 74 Bonati C, D'Elia M, Negro F, et al. Curvature of the pseudocritical line in QCD: Taylor expansion matches analytic continuation[J]. Physical Review D, 2018, **98**(5): 054510.
- 75 Bazavov A, Ding H T, Hegde P, et al. Chiral crossover in QCD at zero and non-zero chemical potentials[J]. Physics Letters B, 2019, **795**: 15 - 21.
- 76 Borsanyi S, Fodor Z, Guenther J N, et al. QCD crossover at finite chemical potential from lattice simulations[J]. Physical Review Letters, 2020, **125**(5): 052001. DOI: 10.1103/PhysRevLett.125.052001.
- 77 Karsch F. Lattice results on QCD thermodynamics[EB/OL]. 2001: arXiv: hep-ph/0103314. <https://arxiv.org/abs/hep-ph/0103314>.
- 78 de Forcrand P, Philipsen O. The QCD phase diagram for small densities from imaginary chemical potential[J]. Nuclear Physics B, 2002, **642**(1 - 2): 290 - 306. DOI: 10.1016/S0550-3213(02)00626-0.
- 79 Borsanyi S, Endrődi G, Fodor Z, et al. The QCD equation of state with dynamical quarks[J]. Journal of High Energy Physics, 2010, **2010**(11): 1 - 33.
- 80 Bazavov A, Bhattacharya T, DeTar C, et al. Equation of state in (2+1)-flavor QCD[J]. Physical Review D, 2014, **90**(9): 094503. DOI: 10.1103/physrevd.90.094503.
- 81 de Forcrand P, Langelage J, Philipsen O, et al. Lattice QCD phase diagram in and away from the strong coupling limit[J]. Physical Review Letters, 2014, **113**(15): 152002. DOI: 10.1103/PhysRevLett.113.152002.
- 82 Maris P, Roberts C D. Dyson-Schwinger equations: a tool for hadron physics[J]. International Journal of Modern Physics E, 2003, **12**(3): 297 - 365. DOI: 10.1142/s0218301303001326.
- 83 Binosi D, Papavassiliou J. Pinch technique: theory and applications[J]. Physics Reports, 2009, **479**(1 - 6): 1 - 152. DOI: 10.1016/j.physrep.2009.05.001.
- 84 Eichmann G, Sanchis-Alepuz H, Williams R, et al. Baryons as relativistic three-quark bound states[J]. Progress in Particle and Nuclear Physics, 2016, **91**: 1.
- 85 Pawłowski J M. Aspects of the functional renormalisation group[J]. Annals of Physics, 2007, **322**(12): 2831 - 2915. DOI: 10.1016/j.aop.2007.01.007.

- 86 Qin S X, Chang L, Chen H, *et al.* Phase diagram and critical end point for strongly interacting quarks[J]. Physical Review Letters, 2011, **106**(17): 172301. DOI: 10.1103/PhysRevLett.106.172301.
- 87 Fu W J, Pawłowski J M, Rennecke F. QCD phase structure at finite temperature and density[J]. Physical Review D, 2020, **101**(5): 054032. DOI: 10.1103/physrevd.101.054032.
- 88 Gao F, Pawłowski J M. QCD phase structure from functional methods[J]. Physical Review D, 2020, **102**(3): 034027. DOI: 10.1103/physrevd.102.034027.
- 89 Gao F, Pawłowski J M. QCD phase structure from functional methods[J]. Physical Review D, 2020, **102**(3): 034027. DOI: 10.1103/physrevd.102.034027.
- 90 Tang C, Gao F, Liu Y X. Practical scheme from QCD to phenomena via Dyson-Schwinger equations[J]. Physical Review D, 2019, **100**(5): 056001. DOI: 10.1103/physrevd.100.056001.
- 91 Fischer C S, Williams R. Probing the gluon self-interaction in light mesons[J]. Physical Review Letters, 2009, **103**(12): 122001. DOI: 10.1103/PhysRevLett.103.122001.
- 92 Cyrol A K, Fister L, Mitter M, *et al.* Landau gauge Yang-Mills correlation functions[J]. Physical Review D, 2016, **94**(5): 054005. DOI: 10.1103/physrevd.94.054005.
- 93 Gao F, Papavassiliou J, Pawłowski J M. Fully coupled functional equations for the quark sector of QCD[J]. Physical Review D, 2021, **103**(9): 094013. DOI: 10.1103/physrevd.103.094013.
- 94 Chang L, Liu Y X, Roberts C D. Dressed-quark anomalous magnetic moments[J]. Physical Review Letters, 2011, **106**(7): 072001. DOI: 10.1103/PhysRevLett.106.072001.
- 95 Qin S, Chang L, Liu Y, *et al.* Practical corollaries of transverse Ward-Green-Takahashi identities[J]. Physics Letters B, 2013, **722**(4 – 5): 384 – 388. DOI: 10.1016/j.physletb.2013.04.034.
- 96 Gao F, Yamada M. Determining wave equations in holographic QCD from Wilsonian renormalization group [J]. Physical Review D, 2022, **106**(12): 126003. DOI: 10.1103/physrevd.106.126003.
- 97 Binosi D, Mezrag C, Papavassiliou J, *et al.* Process-independent strong running coupling[J]. Physical Review D, 2017, **96**(5): 054026. DOI: 10.1103/physrevd.96.054026.
- 98 Deur A, Brodsky S J, de Téramond G F. The QCD running coupling[J]. Progress in Particle and Nuclear Physics, 2016, **90**: 1 – 74.
- 99 Roberts C D, Williams A G. Dyson-Schwinger equations and their application to hadronic physics[J]. Progress in Particle and Nuclear Physics, 1994, **33**: 477 – 575. DOI: 10.1016/0146-6410(94)90049-3.
- 100 Chen L F, Bai Z, Gao F, *et al.* New insight on the quark condensate beyond the chiral limit[J]. Physical Review D, 2021, **104**(9): 094041. DOI: 10.1103/physrevd.104.094041.
- 101 Gao F, Liu Y X. QCD phase transitions via a refined truncation of Dyson-Schwinger equations[J]. Physical Review D, 2016, **94**(7): 076009. DOI: 10.1103/physrevd.94.076009.
- 102 Xin X Y, Qin S X, Liu Y X. Quark number fluctuations at finite temperature and finite chemical potential via the Dyson-Schwinger equation approach[J]. Physical Review D, 2014, **90**(7): 076006. DOI: 10.1103/physrevd.90.076006.
- 103 Lu Y, Chen M Y, Bai Z, *et al.* Chemical freeze-out parameters via a nonperturbative QCD approach[J]. Physical Review D, 2022, **105**(3): 034012. DOI: 10.1103/physrevd.105.034012.